Al-Azhar Engineering 16th International Conference

Vol. 19, No. 72, July 2024, 1 - 19

# DESIGN, MODELING, SIMULATION AND INVESTIGATION OF THE DYNAMIC BEHAVIOR OF A HYDROSTATIC POWER TRANSMISSION SYSTEM FOR HORIZONTAL AXIS WIND TURBINE

**M. Gomaa Aboalnagah[1*], Ziad A. Ibrahim[2], M.Elfaisal Elrefaie[1]**

[1]Mechanical engineering department, Faculty of Engineering, Al-Azhar University, Nasr City, 11884, Cairo, Egypt

[2] Mechanical engineering department, Faculty of Engineering ,Future University, Cairo, Egypt

*Correspondence: Mohamedaboalnaga89@gmail.com

**Citation:**

M.G. Aboalnagah , Z.A. Ibrahim and M.E. Elrefaie, "Design, Modeling, Simulation and Investigation of the Dynamic Behavior of a Hydrostatic Power Transmission System for Horizontal Axis Wind Turbine", Journal of Al-Azhar University Engineering Sector, vol. 1, pp. 1 - 19, 2024,

**Received: 28 October 2023**

**Revised: 02 December 2023**

**Accepted: 11 December 2023**

DOI:10.21608/auej.2023.250831.1484



## ABSTRACT

The basic elements of a traditional wind turbine are installed at the top of the turbine tower. The masses of these elements, together with the forces exerted by wind streams over the turbine blades, represent a heavy load on the turbine tower and require a high-rigidity tower. One of the major elements of a traditional wind turbine is a gear box. The rigid gearbox is squeezed due to turbine rotor driving torque and generator braking torque. The cyclic squeezing process leads to high failure rates for gear boxes, increased maintenance costs, and consequently, lower system reliability. Another issue with conventional wind turbines is that the wind speed is variable, resulting in fluctuating generator rotational speeds. This fluctuation requires a frequency converter to synchronize the generator speed with the electrical grid requirements. This research presents a proposed design of the hydraulic power system for wind turbines to eliminate the above-mentioned problems. The suggested system can seamlessly replace the classical transmission in traditional wind turbines without lowering the turbine performance or other satisfaction criteria. This study introduces a mathematical model for the proposed system components, and a dynamic model is constructed using MATLAB/SIMULINK. The turbine performance is investigated in different conditions, considering factors such as wind speed variation, generator load fluctuation, transmission line length, and accumulator size. The results indicate that the steady-state generator angular speed is almost constant regardless of load or wind speed variations. Moreover, the length of the high-pressure transmission line and the accumulator size significantly influence system dynamics.

**KEYWORDS**: Hydraulic wind turbine, Proportional flow control valve, MATLAB Simulink, Mathematical model, Hydrostatic transmission

## *تصميم ونمذجة ومحاكاة ودراسة السلوك الديناميكي لنظام نقل الطاقة الهيدروستاتيكي لتوربينات الرياح ذات المحور الأفقي*

**محمد جمعه أبوالنجاه[1*]، زياد أحمد إبراهيم[2]، محمد الفيصل الرفاعي[1]**

[1]قسم الهندسة الميكانيكة ، كلية الهندسة، جامعة الأزهر، مدينة نصر، 11884، القاهرة، مصر.

[2]قسم الهندسة الميكانيكة ، كلية الهندسة، جامعة المستقبل ، القاهرة، مصر.

*البريد الاليكتروني للباحث الرئيسي : Mohamedaboalnaga89@gmail.com

## الملخص

عادةً ما توجد المكونات الأساسية لنظام توربينات الرياح التقليدية فوق برج التوربينات. تمثل كتل هذه العناصر إلى جانب القوى التي تنتج من سريان الرياح على ريش التوربينات حملاً كبيرًا على برج التوربين، مما يستلزم وجود برج ذو صلابة عالية. أحد

المكونات الرئيسية في توربينات الرياح التقليدية هو صندوق التروس والتي تتعرض للضغط بسبب عزم الدوران الناشئ من دوران ريش التوربين وعزم الدوران الناشئ من المولد الكهربي. تؤدي عملية الضغط الدوري إلي إرتفاع معدلات فشل صندوق التروس، وزيادة تكاليف الصيانة، وبالتالي تقليل موثوقية النظام.هناك مشكلة أخري تتعلق بتوربينات الرياح التقليدية وهي أن سرعات الرياح متغيرة، مما يؤدي إلى تغيير مستمرفي سرعات دوران المولد. يتطلب هذا التقلب محول تردد لمزامنة سرعة المولد مع متطلبات الشبكة الكهربائية. يقدم هذا البحث تصميم مقترح لنظام الطاقة الهيدروليكية لتوربينات الرياح للتخفيف من المشاكل المذكورة أعلاه. يمكن للنظام المقترح أن يحل محل ناقل الحركة الميكانيكي الكلاسيكي في توربينات الرياح التقليدية بسلاسة دون المساس بأداء التوربينات أو تلبية معايير الرضا الأخرى تقدم هذه الدراسة نموذجًا رياضيًا لمكونات النظام المقترح، كما تم إنشاء نموذج ديناميكي باستخدام حزمة MATLAB/SIMULINK. تم فحص أداء التوربينات في ظروف مختلفة، مع الأخذ في الاعتبار عوامل مثل اختلاف سرعة الرياح، وتقلب حمل المولد الكهربي، وطول خط نقل مائع التشغيل ، وحجم المركم. تشير النتائج إلى أن السرعة الزاوية للمولد الكهربي في حالة الأستقرار تظل ثابتة تقريبًا بغض النظر عن تغيرات حمل المولد الكهربي أو سرعة الرياح. علاوة على ذلك، فإن أطوال خطوط نقل مائع التشغيل وحجم المراكم يؤثران بشكل كبير على ديناميكيات النظام.

**الكلمات المفتاحية :** توربينات الرياح الهيدروليكية، صمام التحكم في التدفق من النوع التناسبي، MATLAB Simulink، النموذج الرياضي، ناقل الحركة الهيدروستاتيكي.

## 1. INTRODUCTION

A wind turbine is one of the renewable energy sources. Normally, the kinetic energy of the wind is harnessed and transformed into diverse energy forms, such as electricity or mechanical energy. Conventional wind turbines are equipped with a turbine rotor designed to capture wind energy in the form of torque and rotational. The resulting wind power is then transmitted to an electric generator through a mechanical gearbox. As the air stream flows over the turbine blades, it induces rotation in the turbine shaft. To enhance efficiency, a gearbox is utilized to elevate the rotational speed to a level at which the generator can generate electrical power more effectively. The generator frequency and the voltage level are adapted so that the power can be integrated with the power grid. The controller (yaw controller, blade pitch controller) ensures the safe and efficient operation of the wind turbine [1].

The main challenge for researchers is to find technical solutions that are compatible with free market economics, i.e., making wind turbines effectively and economically competitive with other sources of energy.

Besides the development of new technologies in wind turbine manufacture, scientific efforts have made it more magnetize for energy investors around the world. Transferring power via a hydrostatic transmission system in a wind turbine is one of these efforts. This system is applicable to traditional wind turbines with minimal modifications to their existing structures.

The Institute for Fluid Power Drives and Control at Aachen University in Germany (IFAS) spearheaded the development and testing of a hydrostatic drive train designed for 1MW-class wind turbines [2]. Their 1 MW test bench, operational since 2010, facilitates measurements under realistic wind turbine conditions, exploring both static and dynamic behaviors and achieving efficiencies of approximately 85% across a broad power range. A hydraulic wind power transfer system utilizing a proportional flow control valve has been proposed and modeled by Majid Deldar et al. [3]. The dynamics of the system components were studied, nonlinearities were taken into account, and the motor load effect was also studied. The mathematical model of their proposed system captured the major functions of the system under different operating conditions. Antonio Jarquin et al. presented an analysis of a dynamic model for fluid power transmission for five megawatt variable speed wind turbines [4]. The mathematical model for their proposed system was created in MATLAB-SIMULINK and compared with a traditional geared transmission system. They observed the impact of system parameters on system response, including high-pressure hose length and variable displacement motor volumetric efficiency. The results indicated that the operating oil volume in the hydraulic transmission had an important parameter on the first natural frequency, and the dynamics of the transmission pipeline became more pertinent for the longest transmission lines. The results also showed that lowering the hydroulic-motor volumetric efficiency

caused a pressure fluctuation damping. A hydrostatic wind power transfer system utilizing a proportional flow control valve with pressure compensator had been proposed and modeled by Majid Deldar et al [5]. Their model was built by using a mathematical model of the system components. The mathematical model was compared to experimental data. The Primary motor parameter behavior, such as pressure and motor speed, was closed to the date that it was obtained from an experimental setup at different operating conditions. Danop Rajabhandharaks presented a proposal for a hydrostatic transmission power system for wind turbine [6]. The main objective of his research was to develop a control strategy that maximized the power capture from wind to the power produced by a generator. The controlled strategy is based on creating a relationship between pump displacement and wind speed. On the other hand, the motor displacement controller grants a constant motor speed under any operating conditions. The results showed that the system efficiency is mainly affeted by leakage and friction losses in the hydraulic components. The results also showed that the system had a fast and well-damped response, and its efficiency ranged from 79% to 84% at steady state . Johannes Schmitz et al, hade analyzed and evaluated four different drive train concepts [7]. These designs were simulated and investigated at rated power. The results showed the overall efficiency was nearly the same -about 85%. A closed- loop hydraulic wind turbine with an energy storage system was proposed by Liejiang Wei. et al [8]. In their proposed system, the generator angular speed was controlled by controlling the motor displacement to get a constant generator speed regardless of input wind speed variation. The mathematical model of their system components was used to build the simulation program in MATLAB SIMULINK. The dynamic response of the hydraulic wind turbine has been investigated under step-change conditions such as linear wind speed, turbine rotor angular speed, and generator demand power. Zengguang Liu et al, presented a storage-type 600 kW wind turbine with a hybrid hydrostatic transmission [9]. Their proposed system was a combination of an open-loop hydrostatic transmission and a closed-loop one. The dynamic responses of the system under two input step signals, wind speed and wind rotor speed, were simulated. Their paper presented the effect of these two-step inputs on wind power, blade tip speed ratio, closed loop motor speed, motor displacement, and energy storage in a hydraulic accumulator.

## 2. SYSTEM DESCRIPTION

The proposed hydraulic circuit for the studied wind turbine is a closed circuit. **Fig.1**.The proposed concept structure includes components like hydraulic tank to store the sufficient amount of hydraulic liquid, hydraulic fluid filter to prevent small metal or dust particles to enter into the system, hydraulic pump to pressurize the operating fluid and send it to the system, primary pump to make up the operating fluid losses in suction line to avoid cavitation, hydraulic motor to drive the load, flow control valve represented in proportional flow control valve to control of system flow rate regardless load pressure variation or supply pressure variation, direction control valve to control the working fluid path during all process, Non return valve to allow operating fluid to flow in unidirection and prevent it from flowing in another direction, and finally pressure relief valve to protect the system from overpressure.

Generally, the available power from wind is extracted by the turbine rotor in the form of torque and rotational speed .The fixed displacement pump group (P1, P2, P3, and Pp) is coupled to the turbine rotor at the top of the turbine tower. The pumps are used to convert the captured mechanical power into hydraulic power in the form of flow and pressure being delivered to the variable displacement hydro-motor (M) throughout direction control valves (DCV1, DCV2, and DCV3) and proportional flow control valve (PFCV) passing through hydraulic hoses or pipes. The motor, in turn, converts the hydraulic power back into mechanical power to drive the electric generator connected to its shaft end at ground level. The main challenge with these proposed design is to get constant generator rotational speed to match them to electrical power grid requirements regardless of wind speed variation and demand power variation. PFCV is achieved these function.

Using a variable- displacement motor allows coverage with wide varying wind speeds. A hydraulic accumulator (ACC.) is installed to protect a high-pressure line against pressure shocks.

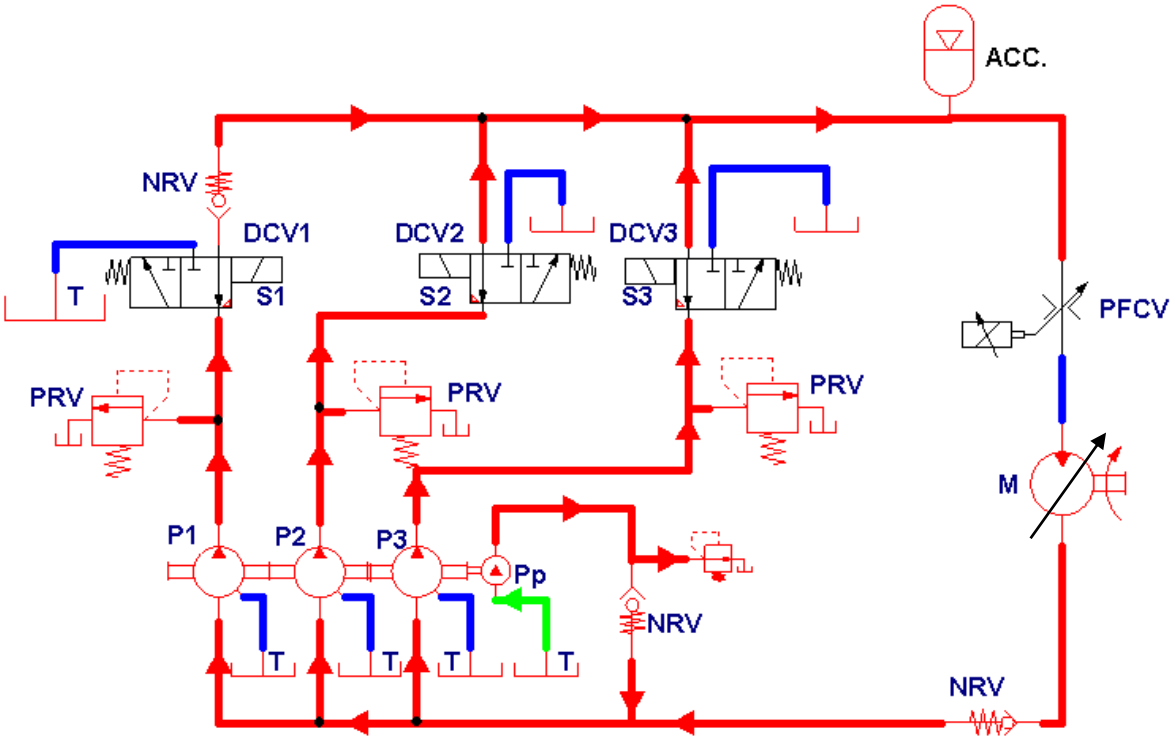


**Fig.1.** Hydraulic circuit schematic

## 3. HYDRO-MECHANICAL SYSTEM ARCHITECTURE

The requirements of the hydraulic transmission system components are based upon the selected wind turbine requirements. In order to choose the suitable components (size and ratio design), the drive system demands must be specified. The performance requirements of a selected wind turbine are maximum torque, minimum speed, and maximum speed. Hence, the hydro-mechanical system is limited by maximum torque and maximum power. The maximum generator torque is limited by the maximum differential pressure across the hydro-motor, while the pump size (pump displacement) is limited by the maximum turbine velocity and the maximum available wind kinetic energy. Turbine speed and generator load have varied over a wide range, these variations are considered for the selection of the system components. The generator should operate normally at a constant speed of 1500 rpm.

The start point for dimensioning the proposed design was the availability of PFCV measurements (Duplomatic QDE5-80/10N-D24K1) [10]. Not all selected valve data for a complete mathematical model was available in manufacturing technical data sheet. Therefore, the missing data can be obtained from direct measurement, disassembly of the valve, and conducting the necessary measurements.

From the above analysis, three fixed displacement axial piston pump type of A2FO, size each 1000cm$^3$/rev, and are directly coupled to the turbine rotor output shaft located above the turbine tower, as shown in **Figure 2**. A variable displacement hydro-motor type A6VM is attached to the generator input shaft at ground level, size 80 cm$^3$/rev.

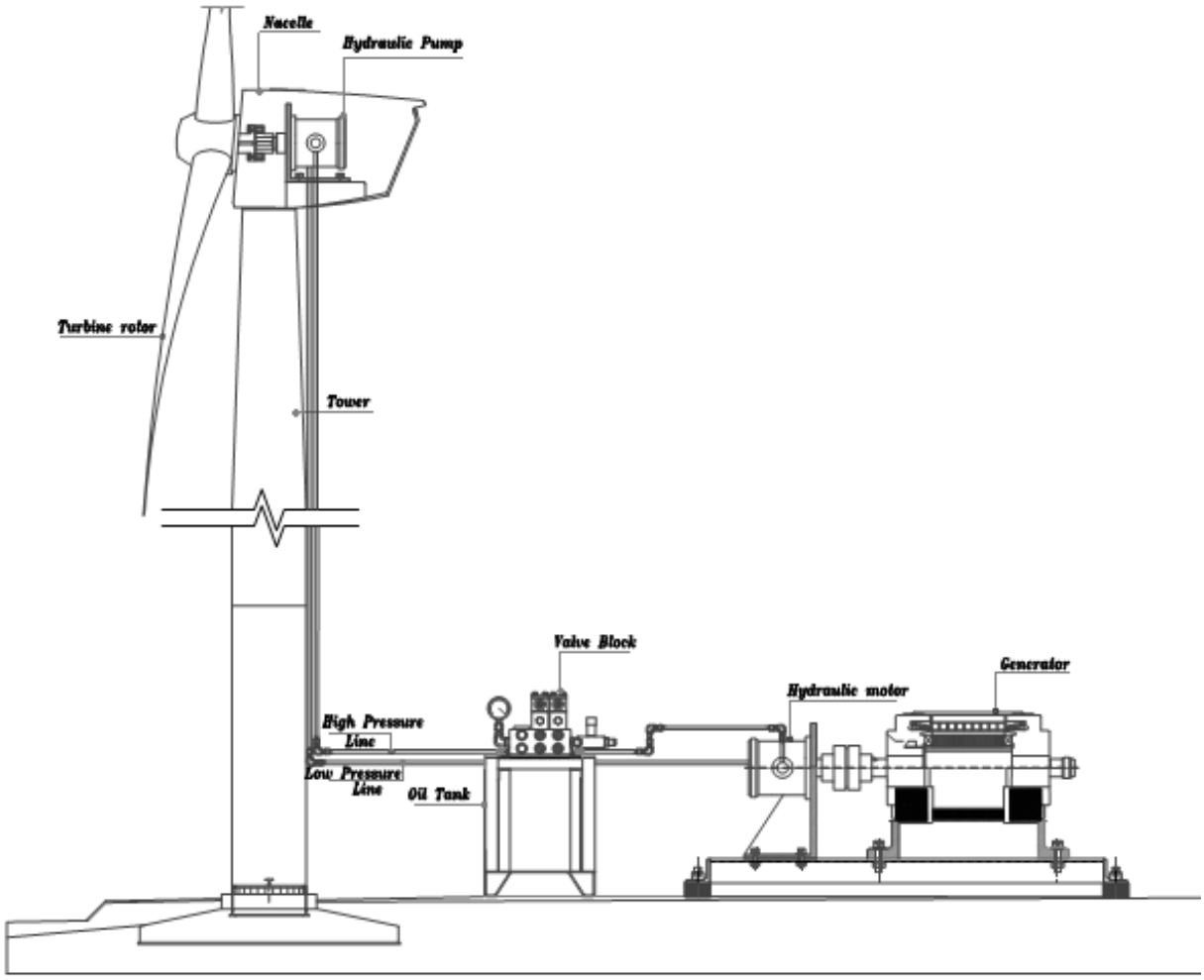


**Fig.2.** Hydro-mechanical system Architecture

## 4. MATHEMATICAL MODEL

In order to complete the modeling of the proposed system for wind turbines, models for a hydraulic system components should be built in.

### 4.1. Pump & Motor Model

Hydraulic pumps serve the purpose of augmenting the energy of the liquid passing through them, operating to increase its energy level. In contrast, the role of hydraulic motors is the reverse of that of the pump, hydraulic motors are displacement machines that transform the received hydraulic power into mechanical output power.

The real pump flow rate is given by:

$$Q_{pa} = V_p \,.\, n_p \; - \frac{P_p}{R_{Lp}} \tag{1}$$

The motor flow rate,

$$Q_m = V_m .\, n_m \; + \frac{P_m}{R_{Lm}} \tag{2}$$

Applying the torque balance equation based on hydraulic motor driving torque and braking torque applied to the hydraulic motor:

$$T_m \; - T_L - T_V - I_m \; \frac{d\omega_m}{dt} = 0 \tag{3.A}$$

Torque balance equation can be rewritten as following:

$$\frac{V_m \,.\, \Delta P_m}{2\pi} \; \eta_{h,m} .\eta_{m,m} - T_L - B_v \,.\, \omega_m - I_m \,.\, \frac{d\omega_m}{dt} = 0 \tag{3}$$

### 4.2. Valves Model

Flow rate through the direction control valve DCV is:

$$Q_{PA} = \sqrt{(P_p - P_{pA})/R_{PA}} \quad (4)$$

The flow rate through the pressure relief valve is:

$$Q_{RV} = \begin{cases} 0 & P_p \leq P_r \\ Q_{RV}(P_p) & P_p > P_r \end{cases} \quad (5)$$

### 4.2.1 Proportional Flow Control Valve

The selected pressure-compensated proportional flow control valve feature a 3- way function. **Fig.3.** [10]. This valve has the ability to control the system flow rate regardless of load pressure variation or supply pressure variation [11 - 16].The flow rate is controllable by an electrical input command signal.

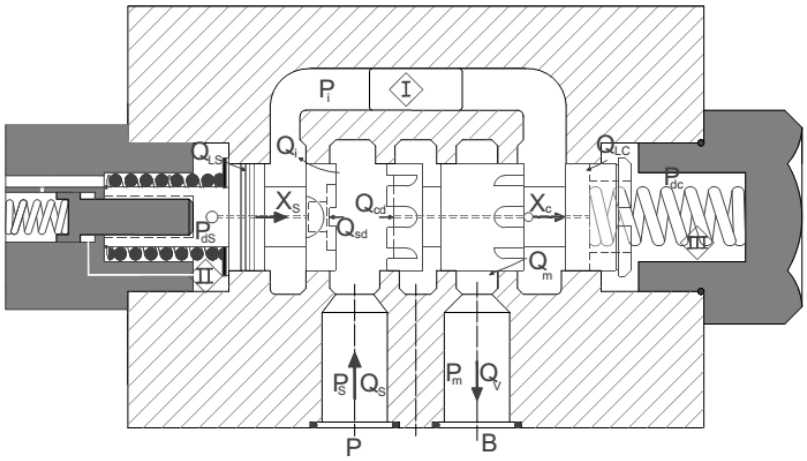


**Fig.3.** Schematic of the proportional flow control valve

The equations describing the dynamic behavior of the selected element are deduced as following,

The valve spool, core, and compensator spool move under the action of the spring forces ($F_{se}, F_{ss}, F_{sc}$), seat reaction forces ($F_{SR1}, F_{SR2}, F_{SR3}, F_{SR4}$)pressure forces ($F_{Ps}$ $F_{bs}$, $F_{bc}$), viscous friction force ($F_{ef}, F_{sf}, F_{cf}$).and the solenoid force applied to the core ($F_e$), **Fig.4**.

**The dynamic equations of motion are giving by the following equations:**

$$\frac{d^2X_e}{dt^2} = \frac{1}{m_e}[F_e - F_{SR1} - F_{SR3} - F_{ef} + F_{se}] \quad (6)$$

$$\frac{d^2X_s}{dt^2} = \frac{1}{m_s}[F_{bs} + F_{SR3} + F_{SR2} - F_{ss} - F_{Ps} - F_{Sf}] \quad (7)$$

$$\frac{d^2X_c}{dt^2} = \frac{1}{m_c}[F_{Ps} + F_{SR4} - F_{bc} - F_{Sc} - F_{cf}] \quad (8)$$

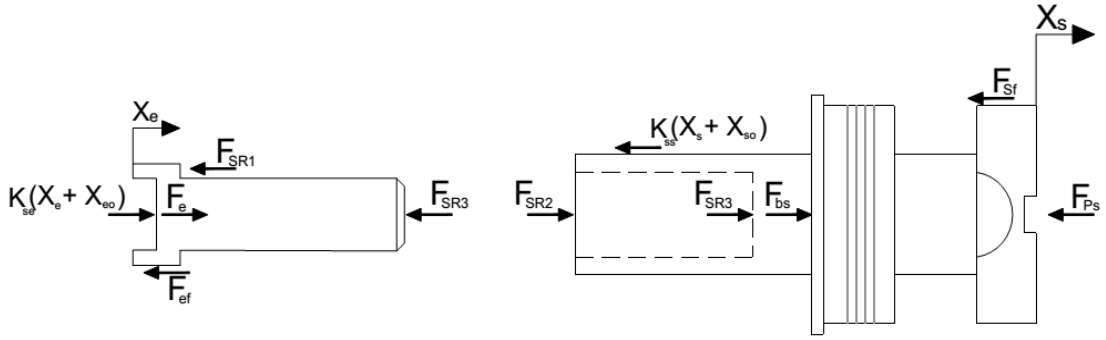

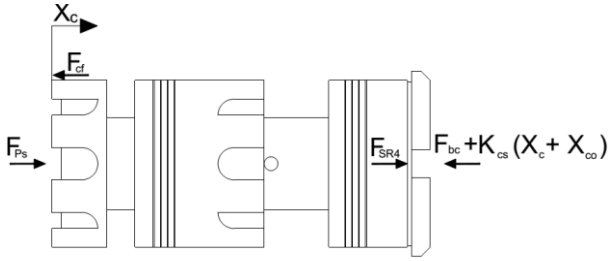


**Fig.4**. Free body diagram of the valve spool and solenoid core(A), Compensator spool(B)

**Solenoid force applied to the core ($F_e$) can be obtained from the following transfer function** [17, 18] :

$$F_e(s)=G*\frac{{\omega_n}^2}{S^2+2\zeta\omega_n S+{\omega_n}^2}\ I(s) \quad (9)$$

**Spring forces acting on the valve spool, compensator, and valve core are given by the following equations:**

$$F_{Se} = K_{se}\ (X_e + X_{e0}) \quad (10)$$

$$F_{SS}= K_{ss}\ (X_s + X_{s0}) \quad (11)$$

$$F_{Sc}= K_{cs}\ (X_c + X_{c0}) \quad (12)$$

**Seat reaction forces acting on the valve spool, compensator, and valve core are given by the following equations:**

$$F_{SR1}=\begin{cases} 0 & X_e \le \text{stroke} \\ K\,|X_e| - R\frac{dX_e}{dt} & X_e \ge \text{stroke} \end{cases} \quad (13)$$

$$F_{SR2}=\begin{cases} 0 & X_s \ge 0 \\ K\,|X_s| - R\frac{dX_s}{dt} & X_s \le 0 \end{cases} \quad (14)$$

$$F_{SR3}=\begin{cases} 0 & X_e < X_s \\ K\,|X_e - X_s| + R\frac{d(X_e - X_s)}{dt} & X_e \ge X_s \end{cases} \quad (15)$$

$$F_{SR4}=\begin{cases} 0 & X_c \ge 0 \\ K\,|X_c| - R\frac{dX_c}{dt} & X_c \le 0 \end{cases} \quad (16)$$

**Pressure forces acting on the valve spool and compensator are given by the following equations:**

$$F_{Ps}= P_s\ .A_s \qquad , A_s = \frac{\pi}{4}(D_s)^2 \quad (17)$$

$$F_{bs}= P_{ds}\ .A_s \quad (18)$$

$$F_{Pc}= P_s\ .A_c \qquad , A_c = \frac{\pi}{4}(D_c)^2 \quad (19)$$

$$F_{bc} = P_{dc} . A_{oc} \quad , \; A_{oc} = \frac{\pi}{4}(D_c)^2 \tag{20}$$

**Valve spool, compensator, and valve core viscous friction forces are given by the following equations:**

$$F_{sf} = f\frac{dX_s}{dt} \quad \text{, where } f = \mu\frac{A_{ps}}{c} \text{ , } A_{ps} = \pi D_s L_{sh} \tag{21}$$

$$F_{cf} = f\frac{dX_c}{dt} \quad \text{, where } f = \mu\frac{A_{pc}}{c} \text{, } A_{pc} = \pi D_c L_{ch} \tag{22}$$

$$F_{ef} = f\frac{dX_e}{dt} \quad \text{, where } f = \mu\frac{A_{pe}}{c} \text{, } A_{pe} = \pi D_e L_{eh} \tag{23}$$

**Throttling areas are calculated as follows:**

The spool and compensator restriction are machined such that the area opened is of a half-circle shape. **Figs. 5A** and **5B**. Shows one of four orifices that represent the area $A_i$ and one of eight orifices that represent the area $A_o$, respectively. The opened area is deduced as follows:

$$A_i = \pi {r_i}^2 . \frac{\theta}{360} - (r_i - X_s)\sqrt{{r_i}^2 - (r_i - X_s)^2} \tag{24A}$$

$$A_i = \begin{cases} 0 & X_s \le X_d \\ 4\left[\frac{\pi {r_i}^2}{180} . \cos^{-1}\left(\frac{(r_i - X_s}{r_i}\right) - (r_i - X_s)\sqrt{2r_i X_s - {X_s}^2}\right] & X_s \ge X_d \end{cases} \tag{24}$$

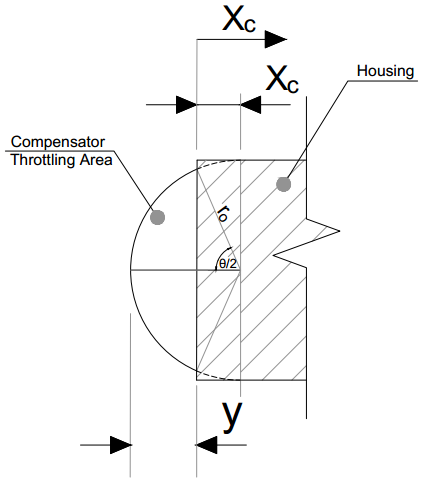


**Fig.5B**. Pressure compensator restriction area

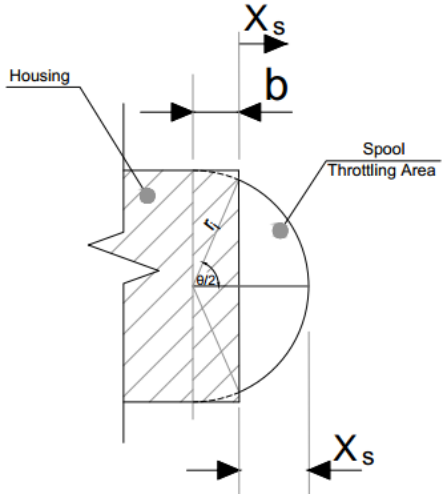


**Fig.5A**. valve spool throttling area

$$A_o = \pi {r_o}^2 . \frac{\theta}{360} - X_c\sqrt{{r_o}^2 - {X_c}^2} \tag{25A}$$

$$A_o = \begin{cases} 0 & X_c \ge r_O \\ 8\left[\frac{\pi . r^2}{180} . \cos^{-1}\left(\frac{X_c}{r}\right) - X_c\sqrt{r^2 - {X_c}^2}\right] & X_c \le r_O \end{cases} \tag{25}$$

**The flow rates through the valve areas are given by the following equations:**

The operating fluid, which flows from the valve spool restriction to the valve exit through the intermediate chamber, can be written as follows:

$$Q_i = C_d . A_i \sqrt{\frac{2}{\rho}(Ps - Pi)} \tag{26}$$

The operating fluid flows from the intermediate chamber to the valve exit through compensator spool throttling. The flow rate through these restrictions, $Q_m$, is given by the following equation:

$$Q_m = C_d \cdot A_o \sqrt{\frac{2}{\rho}(Pi - Pm)} \quad (27)$$

The spool damping orifice is also a short tube orifice. The flow rate through this orifice is given by the following equation:

$$Q_{sd} = \frac{\pi . d_{sd}^4}{128 \mu . L_{sd}} (P_s - P_{ds}) \quad (28)$$

The compensator damping orifice is a short tube orifice. **Fig.6**.The flow rates through the compensator damping orifice from the inlet chamber to the intermediate chamber and downstream compensator spring chamber are deduced as follows:

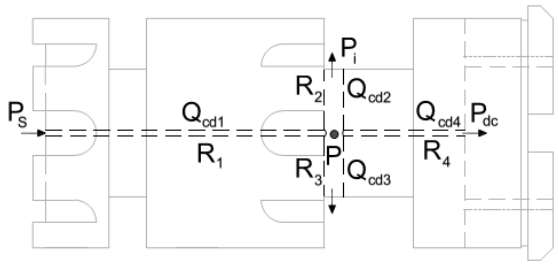


**Fig. 6**. Compensator spool damping holes details

$$Q_{cd1} = Q_{cd2} + Q_{cd3} + Q_{cd4} \quad (29)$$

$$\Delta P = R.Q \qquad \text{where,} \qquad R = \frac{128\,\mu.L}{\pi.d^4} \quad (30)$$

$$P_s - P_i = R_2 Q_{cd2} + 2R_1 Q_{cd2} + R_1 Q_{cd4} \quad (31)$$

$$P_s - P_{dc} = R_4 Q_{cd4} + 2R_1 Q_{cd2} + R_1 Q_{cd4} \quad (32)$$

Eq. (32) can be rewritten as follows:

$$Q_{cd2} = \frac{1}{2R_1}[(P_s - P_{dc}) - Q_{cd4}(R_1 + R_4)] \quad (33)$$

By substituting Eq. (33) in eq. (31), the following relation is obtained:

$$P_s - P_i = \frac{2R_1 + R_2}{2R_1}[(P_s - P_{dc}) - Q_{cd4}(R_1 + R_4)] + R_1 Q_{cd4} \quad (34A)$$

In rearrangement Eq. (34A), the following relations are obtained:

$$\frac{2R_1}{2R_1 + R_2}(P_s - P_i) = [(P_s - P_{dc}) - Q_{cd4}(R_1 + R_4)] + \frac{2{R_1}^2}{2R_1 + R_2} Q_{cd4} \quad (34B)$$

$$Q_{cd4} = \frac{2R_1 + R_2}{2{R_1}^2 - (2R_1 + R_2)(R_1 + R_4)}\left[\frac{2R_1}{2R_1 + R_2}(P_s - P_i) - (P_s - P_{dc})\right] \quad (34)$$

**The leakage flow rate is given by the following equations:**

Internal leakage in hydraulic elements is one of the problems resulting from operating at high pressure levels and the increased clearances due to wear. The leakage flow rate through the clearance between the spool and valve housing is given by:

$$Q_{Ls} = \frac{\pi . D_s\, C^3}{12\,\mu . L_{sh}} (P_{ds} - P_i) \quad (35)$$

The leakage flow rate through the clearance between the pressure compensator and valve housing is given by:

$$Q_{Lc}= \frac{\pi.D_c\, C^3}{12\,\mu.L_{ch}} (P_{dc} - P_i) \quad (36)$$

**The continuity equations applied to the valve chambers are given by the following equations:**

The continuity equation is applied to the intermediate chamber (I) (**Fig. 3**) as follows:

$$\frac{dP_i}{dt} = (\frac{B}{V_i}) * [\, Q_i + 2Q_{cd2} + Q_{Ls} + Q_{Lc} - Q_m - Q_{cd4}] \quad (37)$$

The continuity equation is applied to the downstream spool spring chamber (II) (**Fig.3**) as follows:

$$\frac{dP_{ds}}{dt} = (\frac{B}{V_{bs} - As.Xs}) [\, Q_{sd} - Q_{Ls} + A_s.\frac{dX_s}{dt}\,] \quad (38)$$

The continuity equation is applied to the downstream compensator spring chamber (III) (**Fig.3**) as follows:

$$\frac{dP_{dc}}{dt} = (\frac{B}{V_{bc} - A_c.X_c}) [\, Q_{cd} - Q_{Lc} + A_c\frac{dX_c}{dt}\,] \quad (39)$$

### 4.3 Transmission lines for operating fluid

The operating fluid flowing from the pump to the PFCV through the high-pressure transmission line is moved under the action of fluid inertia, friction, compressibility and pressure forces. **Fig. 7**. The mathematical model for the mentioned system is the lumped parameter model [16]. The four lumped parameter model is closely matched with the behavior of actual flow in pipes.

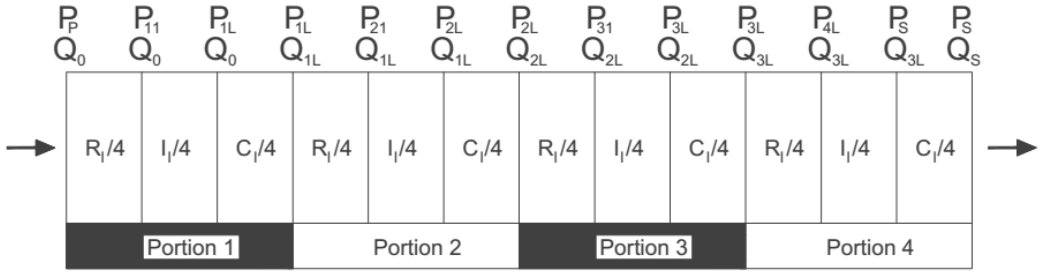


**Fig.7.** Four-lump model

The mathematical model for the four-lump model is described by the following equations:

$$P_p - P_{11} = \frac{R_l}{4} Q_0 \qquad \text{where,} \quad R_l = \frac{128\,\mu\,L}{\pi\, d_t^4} \quad (40)$$

$$P_{11} - P_{1L} = I_l \frac{dQ_0}{dt} \qquad \text{where,} \quad I_l = \frac{4\,\rho\,L}{\pi\, d_t^2} \quad (41)$$

$$Q_0 - Q_{1L} = C_l \frac{dP_{1L}}{dt} \qquad \text{where,} \quad C_l = \frac{\pi\, d_t^4\, L}{4B} \quad (42)$$

Eqs. 40, 41, 42 are repeated in the same manner for portions 2, 3, and 4.Where,

$$Q_s = Q_i + Q_{sd} + Q_{cd1} + A_c\frac{dX_c}{dt} \quad (43)$$

When the accumulator is installed in a high pressure line, the last capacitor (C/4) replaced by the following equation:

$$V_a = V_{oa} - \int (Q_{3L} - Q_S)dt \quad (44)$$

$$P_s = P_{oa}\,(\frac{V_{oa}}{V_a})^n \quad (45)$$

The recommended accumulator size can be calculated using the following eq. [16]:

$$V_{oa} = \frac{n.\rho.A.L.{v_o}^2/2P_{ao}^{1/n}}{\frac{n}{n-1}\left(P_{2a}^{\frac{n-1}{n}} - P_{1a}^{\frac{n-1}{n}}\right) + n\left(P_{1a}.P_{2a}^{\frac{-1}{n}} - P_{1a}^{\frac{n-1}{n}}\right)} \quad (46)$$

Applying the continuity equation between the pump exist and PFCV inlet,

$$Q_{pact} - Q_s - Q_{RV} - \frac{V}{B}\frac{d\,P_{p1}}{dt} = 0 \quad (47)$$

Applying the continuity equation between PFCV exit and hydraulic motor inlet,

$$Q_{PFCV} - Q_m - \frac{V}{B}\frac{d\,P_L}{dt} = 0 \quad (48)$$

## 5. Results and Discussion

The dynamic behavior of a hydrostatic power transmission system for horizontal axis wind turbine is described by equations 1 through 48. These equations were used to develop a computer simulation program using the MATLAB (SIMULINK) package.

The effect of generator braking torque variation on steady-state motor flow rate and electric generator angular speed at rated motor displacement is represented in **Fig.8**. The represented curve is divided into two zones. In the first one (0 to 180 N.m), a pressure-compensated proportional flow control valve, implement the function designed for it and maintain the steady-state motor flow rate almost constant regardless of the continuous rise of generator braking torque. Thus, a constant motor flow rate provided us with a changeless angular generator speed. The first zone has ended at the point at which the compensator in the proportional flow control valve is inactive and the valve is working as a throttling valve. At the mentioned point, the second zone has initiated. In the second zone range, the motor flow rate is uncontrolled, whereas as the generator load increases, the flow rate behavior begins to decrease, and then the generator speed subsequently decrease.

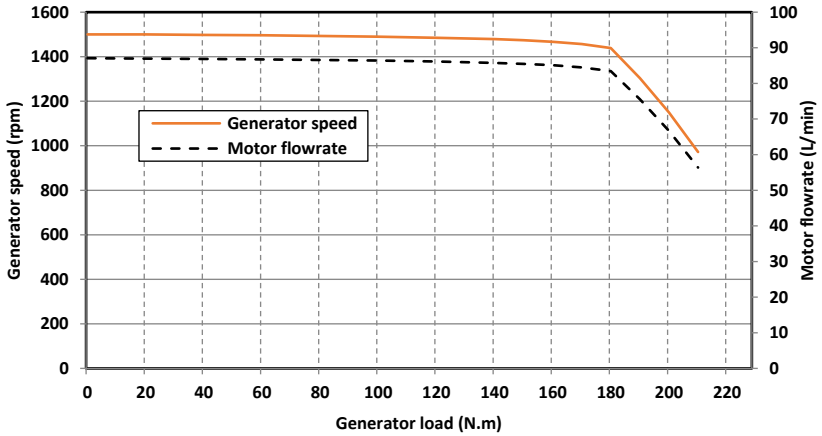


**Fig.8**. Variation generator load with generator speed & motor flow rate

The main control objective of the designed system is to maintain a constant angular speed for the electric synchronous generator. This control objective can be realized by adjusting the hydro-motor displacement side by side with proportional flow control valve position to match the main control objective. As the turbine rotor speed increases, the proportional flow control valve is magnetized to increase the metering area and hence the metering flow rate. As the metering flow rate increases, the motor displacement also increases to get the rated constant angular speed (1500 rpm), as shown in **fig.9**.

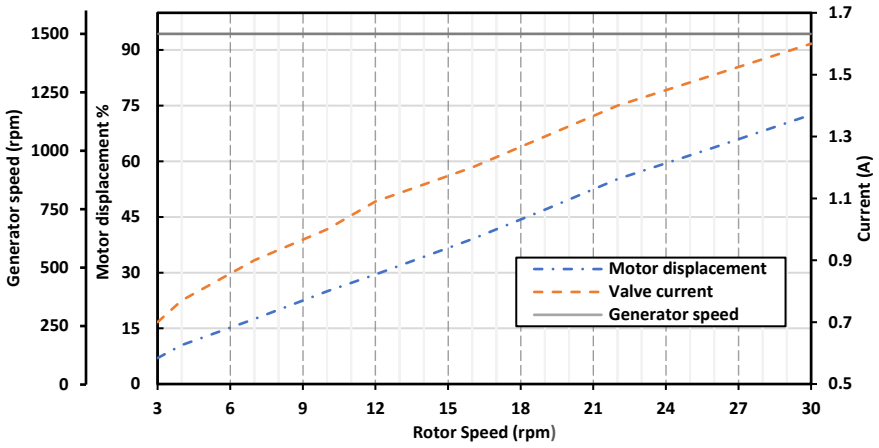


**Fig.9**. Variation of rotor speed with PFCV input current & motor displacement

**Figure 10** presentes and compares the simulated steady-state generator power generation at different generator loads. The represented curve is deduced by adjusting the PFCV spool position and hydraulic motor volumetric efficacy to obtain a constant generator angular speed. The required generator power increases as the generator available load increases, and vice versa. The generation of generator power is limited by the available turbine rotor speed. At arotor speed of 10.5 rpm, the extracted generator powers up to 10 kw at 1500 rpm. The extracted generator power can be increased up to 20 kw and 26 kw at 1500 rpm in the case of available rotor speeds of 23 rpm and 30 rpm, respectively.

The braking generator load is directly proportional to hydraulic motor pressure, whereas as load pressure increases, the required pressure across the hydraulic motor also increases, as shown in **fig.11**. The discussed curve, additionally, **fig. 10**. also indicates that motor pressure differs with the same generator load and hence generator power according to the appropriate motor volumetric efficacy, which is determined according to the available turbine rotor angular speed.

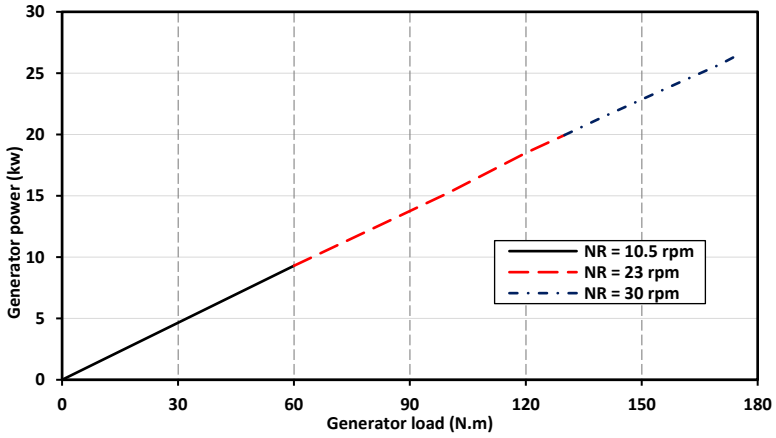


**Fig.10**. Variation of generator load with generator power

The transient time required to give the new steady-state generator speed and generator power as a result of generator load step input is shown in **figs. 12A** and **12B**.The torque pattern presented (**fig. 12A**) is applied to the generator at rated condition. Statically, generator speed and generator power are not affected by load torque variation. A dynamically larger step in torque applied to the generator is required to take a long time (increase settling time) compared to a small step to reach the new balance position again, and vice versa, as shown in **figs. 12A** and **12B**. The mentioned figs also indicated that a larger step in generator torque leads to increased generator speed and generator power overshoot, and vice versa.

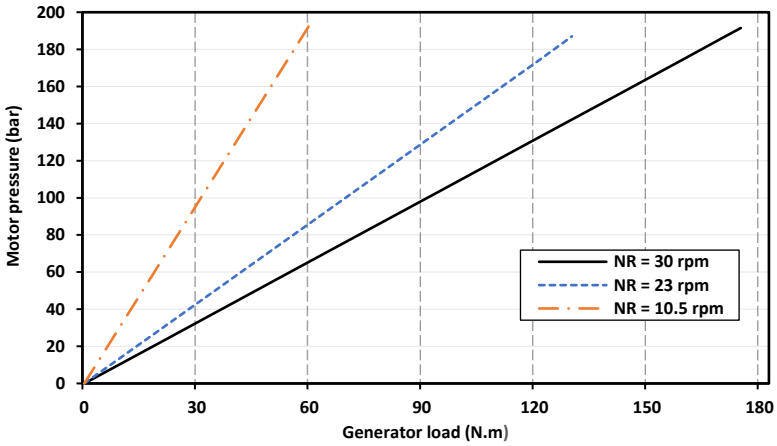


**Fig.11**. Variation of generator load with motor pressure

**Fig. 13**.represents the effect of high pressure line length on the transient response to generator speed. It shows that increasing the pressure line length between the PFCV and hydraulic motor means lowering the subsystem stiffness due to oil compressibility. Hence, increase the transient response, overshoot, and settling time for generator speed, and vice versa. Reduce the transmission line from 1.5 meter to 1 meters and 0.5 meters, reducing the generator speed over shoot and settling time from 46% to 33% and 8%, 0.25 sec to 0.15 sec, and 0.06 sec, respectively. Another marked point is that a long transmission line has a larger volume, hence requiring more filing time then increasing the dead zone. Therefore, the hydraulic motor should be located as close as possible to the PFCV.

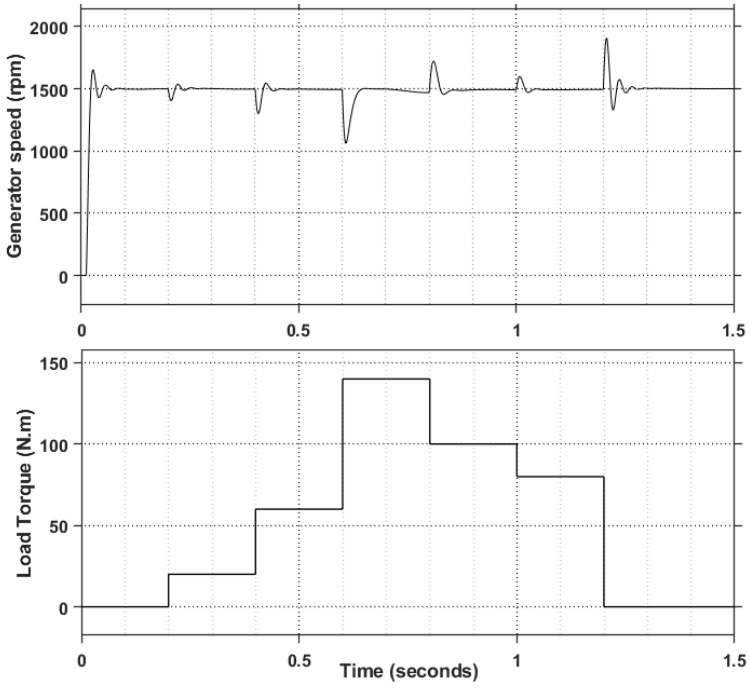


**Fig.12A**. Effect of certain generator load torque on transient response of generator speed

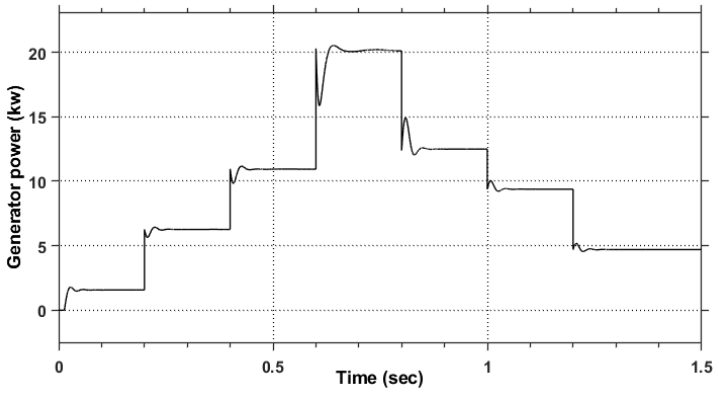


**Fig.12B**. Generator power profile

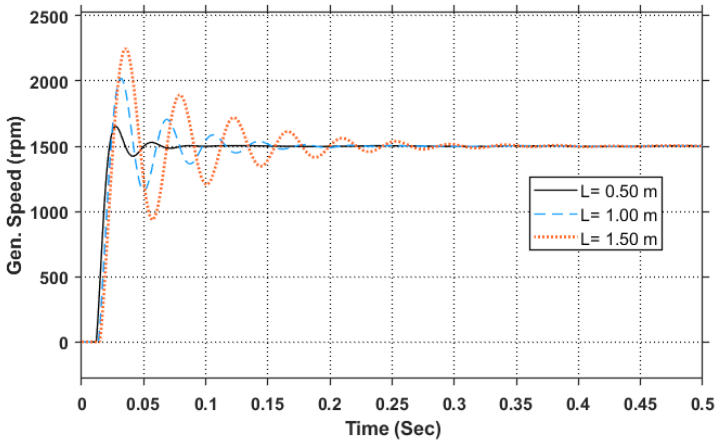


**Fig.13**. Effect of high pressure line length on transient response for generator speed

**Fig. 14** shows that the length of hose connecting the pump and PFCV is insignificant for transient response, overshoot, and settling time for generator speed. The existence of the PFCV and accumulator eliminates the fluctuation in hydraulic generator response. Therefore, the construction of the pump and PFCV at the top of the turbine tower and ground level, respectively, as proposed hydro-mechanical system architecture, matches the previous analysis.

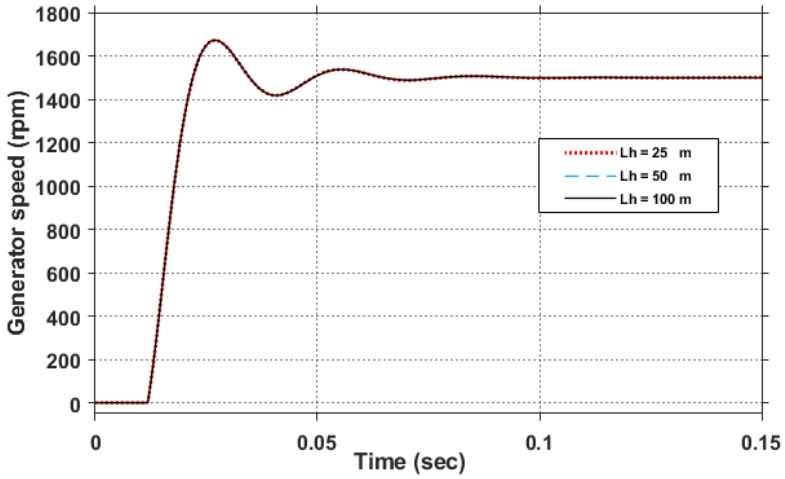


**Fig.14**. Effect of high pressure line length on transient response for generator speed

**Fig.15**. shows the transient response of generator speed in the case of a high-pressure transmission line between the pump group and proportional flow control valve provided by the accumulator with capacities of 0.1 lit and 0.7 lit, and also in the case of the mentioned line not

provided by the accumulator. The presented figure show that the settling times are 1 sec, 0.75 sec, and 0.06 sec for this transmission line without an accumulator and with an accumulator of 0.1 lit and 0.7 lit, respectively. The results also indicate an increase in the accumulator size, an increase in the accumulator capacitance, and a decrease in the system stiffness, thus a more damped response, which provides an increase in the transmission pipe operating life.

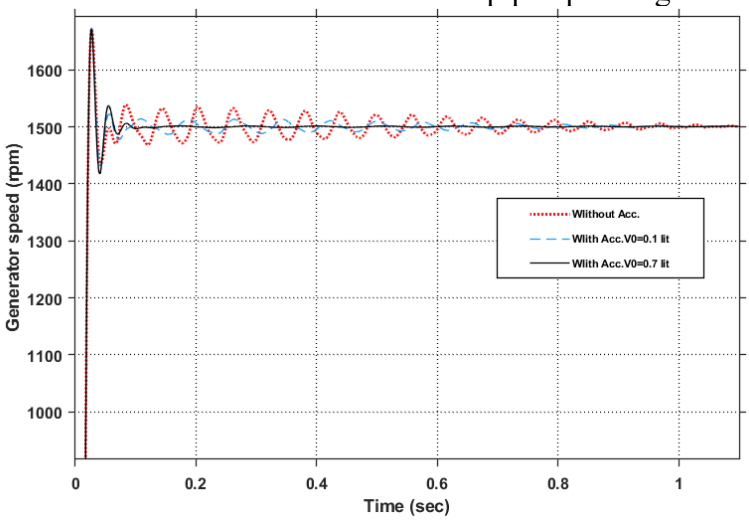


**Fig.15**. Effect of Acc. size on transient response for generator speed

Certain turbine rotor velocity pattern shown in **fig. 16A**. is produced by streaming air flow over turbine blades. As the turbine rotor speed increases (decreases), the flow rate for the coupled pump group also increases (decreases). The presence of a proportional flow control valve set in a suitable position before a hydro-motor grantee controls a constant flow rate and hence a constant electric generator angular speed, as shown in **fig.16.B**. regardless of rotor speed variation. The excess flow rate over rated motor flow passes through the pressure relief valve to the tank.
Statically, turbine rotor speed variation due to varying the air stream speed is not affected on the electric generator angular speed during the controlled zone. A dynamically turbine rotor speed variation at rated condition causes slight local oscillation for a very small time to electric generator angular speed, as shown in **fig.16.A**.

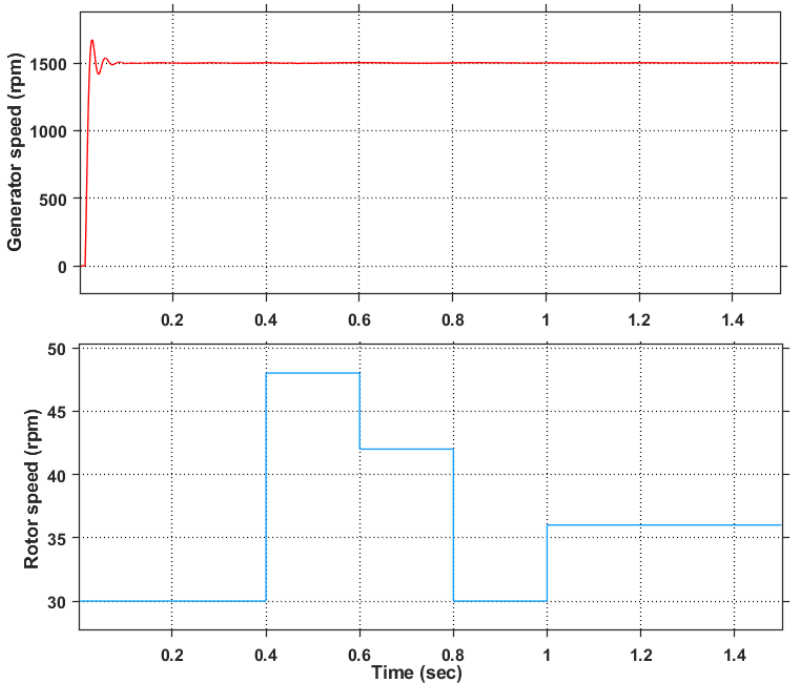


**Fig.16A**. Effect of turbine rotor speed on transient response of generator speed

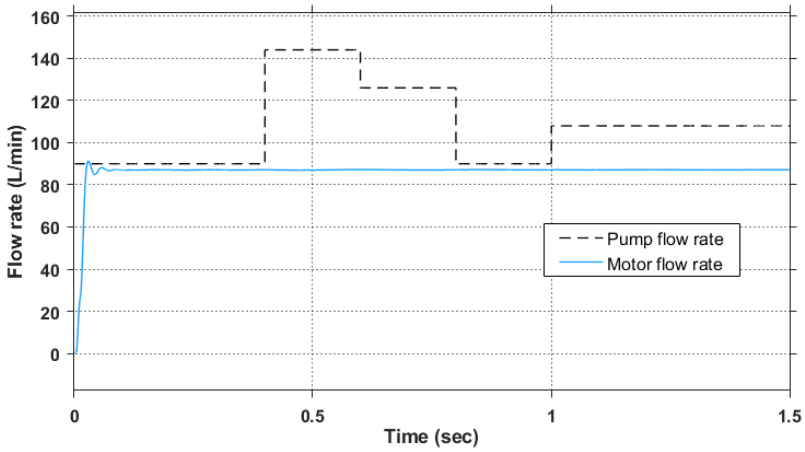


**Fig.16.B**. Effect of turbine rotor speed on steady state pump and motor flow rate

## 6. CONCLUSION

In this research, the classical mechanical drive train in traditional wind turbine systems is replaced by a hydrostatic power transmission system for wind turbines. The automation studio software is used to design the proposed hydraulic circuit that meets the system requirements. This paper introduces a mathematical model for a proposed hydrostatic power transmission system for a horizontal-axis wind turbine. The static and dynamic behavior at different conditions for the designed system is investigated using a simulation program developed by the MATLAB SIMULINK package.The effects of turbine rotor angular speed variation, electric generator load variation, transmission line length, and accumulator size are studied. The results indicate that the steady-state generator angular speed is almost constant regardless of load variation or wind speed variation. An increase in high-pressure transmission line length (between the PFCV and hydraulic motor) causes an increase in overshoot and settling time in generator speed. On the other hand,the transmission line length connecting the pump and PFCV is not significant in system dynamics. The accumulator size is significant for system dynamics. Increasing the accumulator size leads to a decrease in the system stiffness, thus a more damped response. The results also indicate that the variation in angular turbine rotor speed does not affect in generator angular speed.

| | | |
|---|---|---|
| A | Transmission line area | $m^2$ |
| $A_c$ | Compensator cross section area | $m^2$ |
| $A_i$ | Valve spool restriction area | $m^2$ |
| $A_o$ | Compensator restriction area | $m^2$ |
| $A_{pc}$ | Compensator side area | $m^2$ |
| $A_{pe}$ | Core side area | $m^2$ |
| $A_{ps}$ | Valve spool side area | $m^2$ |
| $A_s$ | Valve spool cross section area | $m^2$ |
| B | Bulk modulus of oil | Pa |
| C | Radial Clearance | m |
| $C_d$ | Discharge coefficient | ----- |
| $C_l$ | Transmission line capacitance | $m^3$/pa |
| $D_c$ | Compensator diameter | m |
| $d_{cd}$ | Diameter of compensator damping orifice | m |
| $D_s$ | Valve spool diameter | m |
| $d_{sd}$ | Diameter of valve spool damping orifice | m |
| $d_t$ | Transmission line diameter | m |
| f | Friction coefficient | Ns/m |
| $F_{bc}$ | Downstream pressure force applied on Compensator | N |
| $F_{bs}$ | Downstream pressure force applied on the valve spool | N |
| $F_{cf}$ | Viscous friction force for compensator | N |
| $F_e$ | Solenoid force applied on the core | N |

| | | |
|---|---|---|
| $F_{ef}$ | Viscous friction force for the core | N |
| $F_{Ps}$ | Upstream pressure force applied on the valve spool | N |
| $f_s$ | Spool friction coefficient | N.s/m |
| $F_{sc}$ | Compensator spring force | N |
| $F_{se}$ | Core spring force | N |
| $F_{sf}$ | Viscous friction force for valve spool | N |
| $F_{SR1}$ | Seat reaction force produced by seating the core in core housing | N |
| $F_{SR2}$ | Seat reaction force produced by seating the valve spool in valve housing | N |
| $F_{SR3}$ | Contact force produced by seating the valve spool on core | N |
| $F_{SR4}$ | Seat reaction force produced by seating the compensator on valve housing | |
| $F_{ss}$ | Valve spool spring force | N |
| I | PFCV input current | A |
| $I_l$ | Transmission line inertia | $Kg.m^4$ |
| $I_m$ | Motor inertia | $Kg.m^2$ |
| K | Equivalent seat material stiffness | N/m |
| $K_{cs}$ | Downstream Compensator spring stiffness | N/m |
| $K_{se}$ | Core spring stiffness | N/m |
| $K_{ss}$ | Downstream valve spool spring stiffness | N/m |
| L | Length of transmission line | m |
| $L_{cd}$ | Length of compensator damping orifice | m |
| $L_{ch}$ | Contact distance between compensator and housing | m |
| $L_{eh}$ | Contact distance between valve core and housing | m |
| $L_{sd}$ | Length of valve spool damping orifice | m |
| $L_{sh}$ | Contact distance between valve spool and housing | m |
| $m_c$ | Compensator mass | Kg |
| $m_e$ | Core mass | kg |
| $m_s$ | Valve spool mass | Kg |
| n | Polytropic exponent | ----- |
| $n_m$ | Motor rotating speed | rpm |
| $n_p$ | Pump rotating speed | rpm |
| $P_{1a}$ | Minimum accumulator pressure | Pa |
| $P_{2a}$ | Maximum accumulator pressure | Pa |
| $P_{dc}$ | Pressure in downstream Compensator chamber | Pa |
| $P_{ds}$ | Downstream pressure applied on valve spool | Pa |
| $P_i$ | Pressure in intermediate chamber for valve | Pa |
| $P_m$ | Motor differential pressure | Pa |
| $P_{oa}$ | Accumulator pre charging pressure | Pa |
| $P_p$ | Pump differential pressure | Pa |
| $P_{pA}$ | Pressure at DCV exit | Pa |
| $P_r$ | PRV cracking pressure | Pa |
| $P_s$ | Upstream pressure applied in valve spool | Pa |
| $Q_{cd}$ | Flow rate through compensator damping orifice | $m^3/s$ |
| $Q_i$ | Flow rate through valve spool restriction | $m^3/s$ |
| $Q_{Lc}$ | Leakage flow rate through clearance between compensator and valve housing | $m^3/s$ |
| $Q_{Ls}$ | Leakage flow rate through clearance between valve spool and valve housing | $m^3/s$ |
| $Q_m$ | Motor Flow rate | $m^3/s$ |
| $Q_{pa}$ | Real flow rate for the pump | $m^3/s$ |
| $Q_{PA}$ | Flow rate through DCV | $m^3/s$ |
| $Q_{RV}$ | Flow rate through PRV | $m^3/s$ |
| $Q_{sd}$ | Flow rate through valve spool damping orifice | $m^3/s$ |
| $Q_v$ | PFCV Flow rate | $m^3/s$ |
| R | Equivalent seat material damping coefficient | N. s/m |
| $r_i$ | Radius of spool orifice area | m |
| $R_l$ | Transmission line resistance | $N.s/m^5$ |
| $R_{Lm}$ | Motor resistance to internal leakage | N. s/m |
| $R_{Lp}$ | Pump resistance to internal leakage | N. s/m |
| $r_o$ | Radius of compensator orifice area | m |
| $R_{PA}$ | Resistance in DCV | |
| $T_L$ | Torque applied on hydraulic motor | N.m |
| $T_m$ | Torque produced via hydraulic motor | N.m |
| $T_V$ | Torque required to overcome oil viscosity in hydraulic motor | N.m |
| V | Fluid volume | $m^3$ |

| | | |
|---|---|---|
| $V_a$ | Accumulator volume | $m^3$ |
| $V_{bc}$ | Compensator downstream chamber fluid volume | $m^3$ |
| $V_{bs}$ | Valve spool downstream chamber fluid volume | $m^3$ |
| $V_i$ | Valve intermediate chamber fluid volume | $m^3$ |
| $V_m$ | Motor displacement | $m^3/rev$ |
| $V_{oa}$ | Volume of charging accumulator gas at initial pressure | $m^3$ |
| $V_P$ | Pump displacement | $m^3/rev$ |
| $X_c$ | Compensator displacement | m |
| $X_{co}$ | Initial downstream Compensator spring displacement | m |
| $X_d$ | Spool overlap displacement | m |
| $X_e$ | Core displacement | m |
| $X_{eo}$ | Downstream core spring pre-compression displacement | m |
| $X_s$ | Valve spool displacement | m |
| $X_{so}$ | Downstream valve spring pre-compression displacement | m |
| $\rho$ | Oil density | $Kg/m^3$ |
| $\omega_m$ | Motor angular velocity | Rad/sec |
| $\mu$ | Oil dynamic viscosity coefficient | Pa.s |

## REFERENCES

[1] J.F.Manwell, J.G.Mcgowan, A.L.Rogers,2009.Wind energy explained, theory, design and application.John Wiley Sons Ltd.

[2] J. Schmitz , Vatheuer N., Murrenho H.,2013.Hydrostatic transmissions: A power play in wind turbine design . RWTH Aachen Univ. IFAS Aachen Ger.

[3] D. Majid , Afshine I., Senior M.,Masoud V.,and Sohel A.,2013. A hydraulic wind power transfer system: operating and modeling. IEEE Transactions on Industry Applications.

[4]J. Antonio , Niels F., Jan W.,2014. Analysis of dynamics of fluid power drive-trains for variable speed wind turbines: parameter study. IET Renew. Power Gener., Vol. 8, Iss. 4, pp. 398–410, doi: 10.1049/iet-rpg.2013.0134.

[5] D. Majid , Afshine I., Senior M.,Masoud V.,and Sohel A.,2015. Modeling of a hydraulic wind power transfer system utilizing a proportional flow control valve. IEEE Transactions on Industry Applications, 51(2): 1837–1844

[6] R. Danop,2014 .Control of Hydrostatic Transmission Wind Turbine. Master's Theses. 4513. http://scholarworks.sjsu.edu/etd_theses/4513

[7] S. Johannes, Gunnar M. and Hubertus M.,2014.Hydrostatic transmission for wind turbines – Comparison of different configurations and their applicability. In: Proceeding of the 9th International Fluid Power Conference, pp. 144 – 152, Aachen.

[8] W. Liejiang, Zengguang L., Yuyang Z., Gang W,and Yanhua T. .Modeling and Control of a 600 kW Closed Hydraulic Wind Turbine with an Energy Storage System. Appl. Sci. 2018, 8, 1314; doi:10.3390/app8081314.

[9] L. Zengguang, Yanhua Tao,Liejiang Wei, Peng Zhanand Daling Yue,2019 .Analysis of Dynamic Characteristics of a 600 kW Storage Type Wind Turbine with Hybrid Hydraulic Transmission.Processes 7, 397; doi:10.3390/pr7070397.

[10] https://duplomaticmotionsolution.com.

[11] D.Wu , R.Burton ,G.Schoenau,D.Bitner ,2007, Analysis of pressure-compensated flow control valve.Journal of dynamic systems, measurement ,and control, vol.129,pp.203-211.

[12] D. Derose ,2003. Proportional and servo technology. Fluid power journal March /April2003, pp.8-12.

[13] Mannesmann Rexroth GmbH.Basic principle and components of fluid technology. The hydraulic trainer volume 1, RE00290/10.91,199.

[14] Mannesmann Rexroth GmbH .Proportional and servo technology.The hydraulic trainer volume 2, RE00291/12.89.

[15] M.Cheng ,2005. Modeling and analysis of a pressure compensated flow control valve.Proceeding of FEDSM2005,ASME,Fluid engineering division summer meeting,Houston ,Texas ,USA,Volume 2,pp.17-25.

[16] M.Galal Rabie,2009.Fluid Power Engineering. McGraw-Hill, New York.

[17] S. Wang, Zhidan Weng ,and Bo.Jin ,2020, .A performance improvement strategy for solenoid electromagnetic actuator in servo proportional valve. Appl.sci ,10,4352.

[18] M.F. Badr,2018 .Modeling and simulation of a control solenoid. IOP Conf .series :Material science and engineering 433,012082 .